

Magnetic transitions and electrical transport in lanthanum strontium manganite: Effects of substitutions and high pressure

G. Srinivasan^{a)} and D. Hanna

Physics Department, Oakland University, Rochester, Michigan 48309-4401

(Received 29 March 2001; accepted for publication 1 June 2001)

The observation of a substitution-induced ferromagnetic order ($T_c=200$ K) is reported in antiferromagnetic $\text{La}_{0.9}\text{Sr}_{0.1}\text{MnO}_3$ ($T_N=130$ K) when 0.05 of La is replaced by yttrium. Important results of ferromagnetic resonance (FMR) and high-pressure transport studies are as follows. (i) Data on FMR linewidth and resistivity provide evidence for the presence of microscopic magnetic inhomogeneities, possibly $\text{La}_{0.9}\text{Sr}_{0.1}\text{MnO}_3$. (ii) For zero external pressure, a resistivity peak at 130 K due to intergrain tunneling, a secondary peak close to T_c , and magnetoresistance (MR) on the order of 30% are observed. (iii) At high pressures, the resistivity peaks shift to higher temperatures at the rate of 24–26 K/GPa and MR values decrease. (iv) An internal pressure of 3 GPa due to Y substitution is inferred from high-pressure transport studies. © 2001 American Institute of Physics. [DOI: 10.1063/1.1388872]

This study was aimed at the nature of magnetic interactions in lanthanum manganites through substitutions and the application of an external pressure. The perovskite $\text{La}_{1-x}\text{Sr}_x\text{MnO}_3$ exhibits a variety of magnetic phases.^{1–3} The end member $x=0$ is an antiferromagnetic insulator due to the superexchange between Mn^{3+} ions.¹ The substitution of Sr leads to a ferromagnetic double exchange interaction, metallic conductivity, and a large magnetoresistance (see Ref. 4). The appearance of ferromagnetism is reported for $x=0.1$ and metallic conductivity for $x=0.17$.^{1,2}

The strength of DE interactions depends on the bond angle and bond distance and these structural parameters could be controlled either with partial substitutions for La or by applying external pressure. Trivalent substitutions such as Y^{3+} are preferred since mono or divalent ions change the average valency of Mn and affect the strength of DE.⁵ Since there are three types of A–O bond lengths (corresponding to A=La, Sr, Y) and two different Mn–O bond lengths ($\text{Mn}^{3+}\text{–O}$ and $\text{Mn}^{4+}\text{–O}$) substitution induced changes are somewhat uncontrolled. With external pressure, however, one can introduce a controlled change. Studies on high-pressure effects are therefore ideal for an understanding of the nature of the ferromagnetic DE.

Here we report on the effects of yttrium substitution and high pressure on magnetic and transport properties of $\text{La}_{1-x}\text{Sr}_x\text{MnO}_3$ with the composition of interest, i.e., $x=0.1$ since an antiferromagnetic to ferromagnetic transition and a rapid increase in T_c with x are reported for x values around 0.1.¹ When 0.05 of La is replaced by Y, we observed a 0.6% reduction in volume and an antiferromagnetic ($T_N=130$ K) to ferromagnetic ($T_c=200$ K) transition. Both ferromagnetic resonance (FMR) linewidth and electrical resistivity data provide evidence for the presence of magnetic inhomogeneities, most likely antiferromagnetic clusters with a $T_N=130$ K. A tunnel-type giant magnetoresistance (MR) is observed in the sample. We inferred from high pressure

transport studies a 3 GPa internal pressure due to Y substitution.

Polycrystalline samples of $\text{La}_{0.9}\text{Sr}_{0.1}\text{MnO}_3$ (LSMO) and $\text{La}_{0.85}\text{Y}_{0.05}\text{Sr}_{0.1}\text{MnO}_3$ (LYSMO) were prepared by the standard ceramic techniques. The samples were found to be single phased and orthorhombic. Yttrium substitution resulted in a 0.6% decrease in the unit cell volume. For static magnetic characterization, a Faraday balance was used. Low field susceptibility χ was measured for a field $H=50$ Oe and saturation magnetization M_s was measured with $H=5$ kOe. Figure 1 shows the temperature dependence of χ for powder samples of LSMO and LYSMO. The susceptibility data for LSMO is reminiscent of expected behavior for an antiferromagnet with a Neel temperature T_N of 130 K. We did not observe ferromagnetism in LSMO reported in earlier studies.¹ Yttrium substitution in LSMO leads to the onset of ferromagnetism and a sharp increase in the ordering temperature to 200 K. The measured low temperature M_s for LYSMO is 95 emu/g and is in very good agreement with the expected value of 100 emu/g.⁶

Additional evidence for ferromagnetic order in LYSMO was obtained from FMR studies at an x band on a 100 μm thick disk with the static magnetic field applied parallel to

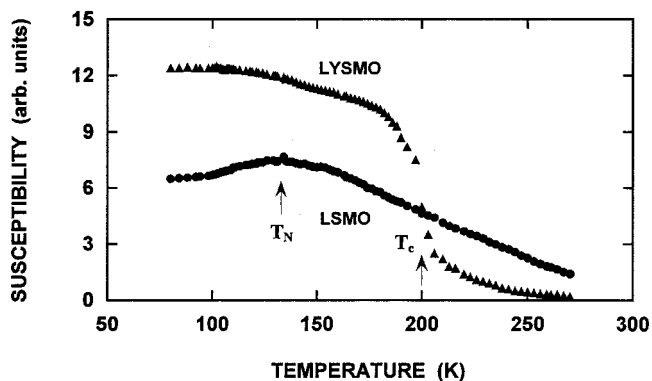


FIG. 1. Susceptibility vs temperature data for $\text{La}_{0.9}\text{Sr}_{0.1}\text{MnO}_3$ (LSMO) and $\text{La}_{0.85}\text{Y}_{0.05}\text{Sr}_{0.1}\text{MnO}_3$ (LYSMO). The arrows indicate the magnetic transition temperatures; $T_N=130$ K for LSMO and $T_c=200$ K for LYSMO.

^{a)}Electronic mail: srinivas@oakland.edu

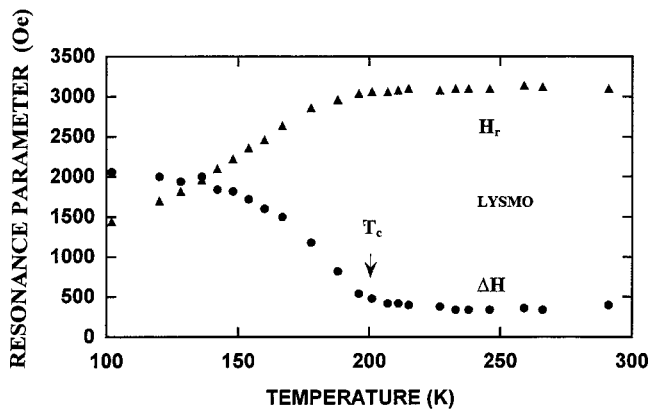


FIG. 2. Ferromagnetic resonance linewidth ΔH and resonance field H_r at 9.2 GHz for a 100 μm thick disk of LYSMO. The arrow indicates the Curie temperature.

the sample plane. Both the linewidth ΔH and the resonance field H_r were measured as a function of temperature and are shown in Fig. 2. As the sample is cooled from room temperature, H_r and ΔH remain constant in the paramagnetic state. The resonance field corresponds to a g value of 2.01, expected for Mn ions. With the onset of ferromagnetism below 200 K, H_r decreases primarily due to contribution from the shape anisotropy. The linewidth increases rapidly from T_c down to 130 K and then stays constant with decreasing temperature.

Consider the temperature dependence of ΔH in the ordered state that shows a 300% increase relative to the paramagnetic state. An increase in ΔH is predicted due to valence exchange which involves the transfer of electrons between Mn^{3+} and Mn^{4+} , slow or fast relaxing impurities, porosity, anisotropy, and eddy currents.^{7,8} However, the 300% increase in ΔH Fig. 2 could only be due spin wave scattering by inhomogeneities. Data on linewidth as a function of temperature is useful for extracting information on the chemical homogeneity of lanthanum manganite films and polycrystalline samples.⁹ Any chemical defects can be modeled as spreads in T_c and M_s . The linewidth is then the sum of the intrinsic part and broadening due to spreads in T_c and M_s . Thus microscopic impurities, most likely LSMO, cause the broadening of the FMR linewidth in Fig. 2. The most significant observation is the sharp drop in ΔH from 130 to 200 K, the ordering temperatures for LSMO and LYSMO, respectively. Further evidence for LSMO-like impurities were obtained from transport data.

Resistivity (ρ) measurements were done with the standard four probe technique for an excitation current of 1 μA at 10 Hz. The magnetoresistance $\text{MR} = [\rho(H) - \rho(0)] / \rho(0)$ was measured for $H = 4$ kOe. For LSMO, the low temperature $\rho(0)$ was on the order of $10^5 \Omega\text{cm}$, ρ vs T behavior was insulator-like, and MR values were quite small. Temperature dependence of $\rho(0)$ and MR are shown in Fig. 3 for LYSMO. With Y substitution, $\rho(0)$ decreases by eight orders of magnitude and a metallic conductivity is observed. With increasing T , a peak in $\rho(0)$ appears at $T_1 = 130$ K, and the shoulder observed at $T_2 = 185$ K is close to the Curie temperature of 200 K. The MR at low temperatures is large, about 30% for a static field of 4 kOe and it decreases with increasing T . The observed metallic conduction is of interest since

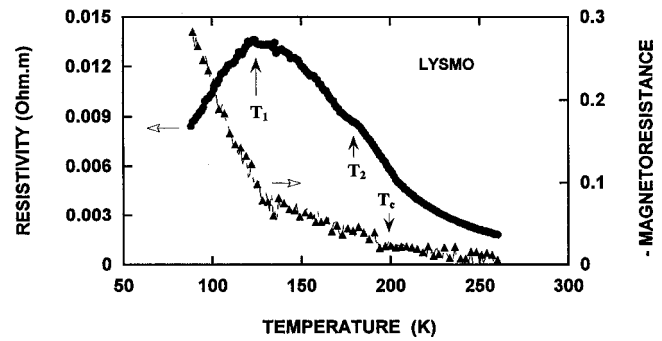


FIG. 3. Temperature dependence of the zero field resistivity and the magnetoresistance (MR) for LYSMO for zero applied pressure. The MR values are for an applied magnetic field of 4 kOe. The arrows indicate the low temperature at T_1 , the shoulder at T_2 and T_c .

$\text{La}_{1-x}\text{Sr}_x\text{MnO}_3$ shows such a behavior at only $x > 0.175$.² It is very likely that Y with an ionic radius of 0.089 nm (versus 0.112 nm for Sr) causes local distortions that enhances the electron-phonon coupling and the onset of metallic conduction.

The most important features in Fig. 3 are the peak at T_1 and the large low temperature MR. A similar low temperature peak and tunneling assisted MR were reported for the granular $\text{La}_{0.85}\text{Sr}_{0.15}\text{MnO}_3$ with the average grain size D ranging from 50 to 200 nm.¹⁰ Resistivity data for $D = 50$ nm showed a broad peak at 225 K ($=T_1$) and a shoulder at 280 K ($=T_2$). As D was increased, the peak at T_1 was progressively suppressed and it finally disappeared for the bulk sample (with a very large D). In order to account for these observations, the authors proposed a model based on the following assumption. The fine grains could be divided into surface and bulk regions, with the surface spins subjected to a relatively weak magnetic interaction due to lack of nearest neighbors and, consequently, a much lower ordering temperature $T_c = T_1$ compared to the interior of the grain with a Curie temperature of T_2 . Theoretical estimates of both ρ and MR based on this model were in excellent agreement with their data.¹⁰ We propose a similar phenomenon in the present LYSMO sample in which magnetic and/or chemical inhomogeneities with an ordering temperature T_1 are present. We further argue that the impurities are most likely antiferromagnetic clusters of LSMO based on the following observations. (i) The resistivity peak occurs at $T_1 = T_N$ for LSMO; (ii) earlier discussion on impurity assisted line broadening of FMR (data in Fig. 2) indicate LSMO-like chemical defects in the sample. The peak in $\rho(0)$ at T_1 in Fig. 3 is not due to a metal-insulator transition. For $T > T_1$, tunneling of charge carriers between the ordered LYSMO regions across the paramagnetic impurities becomes possible, leading to an overall decrease in ρ . Furthermore, the large low temperature MR is also an indicator of tunneling assisted electrical transport.¹⁰

High-pressure transport measurements were carried out on LYSMO samples to study its effect on magnetic interactions and for an estimate of the internal pressure due to chemical substitutions. A Cu-Be liquid pressure cell was used to achieve pressures P as high as 1 GPa and obtain data as in Fig. 3 for a series of pressures. Three important effects are observed at high pressures: (1) ρ decreases with increasing P , (2) the peak at T_1 and the shoulder at T_2 are broad-

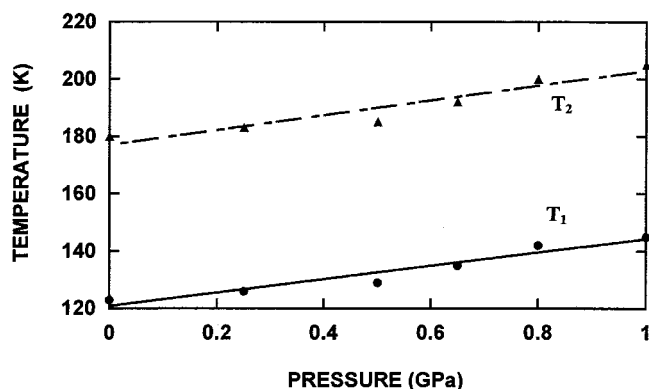


FIG. 4. Variation of T_1 and T_2 with applied hydrostatic pressures P for LYSMO. The data were obtained from resistivity data as in Fig. 3 for pressures up to a maximum of 1 GPa with a liquid pressure cell.

ened and shifted to higher temperatures, and (3) the magnitude of MR decreases. The variation of T_1 and T_2 with P is plotted in Fig. 4. One notices a linear dependence, with an increase of 24 and 26 K/GPa for T_1 and T_2 , respectively. An external pressure affects the bond length $d_{\text{Mn-O}}$ and the bond angle θ and studies on LaNiO_3 show compression of $d_{\text{Mn-O}}$ and increase of θ .¹¹ With nominal values for bond-length and bond-angle compressibilities, theoretical estimates for the sign and magnitude for dT_c/dP in manganites were found to be in reasonable agreement with experimental values.¹² In this study, both T_1 and T_2 have the same rate of increase with P . If we associate T_1 with the an antiferromagnet-like ordering of defects and T_2 with ferromagnetic LYSMO, then it is quite remarkable that both the superexchange and the double exchange have identical dependence on pressure through changes in structural parameters.

Now we compare the effects of substitution and high pressure. A trivalent ion such as Y with a small ionic radius is expected to decrease $d_{\text{Mn-O}}$, but studies also reveal a decrease in θ for Y substitution in lanthanum calcium manganites, leading to an overall decrease in T_c in that system.¹³ In

the present system, however, the ordering temperature increases from 130 to 200 K when Y is substituted for La. Since the strength of DE is much more sensitive to variations in θ than any changes in $d_{\text{Mn-O}}$, it is likely that Y substitution in LSMO results in an increase in bond angle and a decrease in the bond length, effects similar to the application of external pressure. One could infer from the data in Fig. 4 that the 70 K increase in the ordering temperature for LYSMO corresponds to 3 GPa of external pressure.

In conclusion, Y substitution in $\text{La}_{0.9}\text{Sr}_{0.1}\text{MnO}_3$ results in a ferromagnetic metallic state. Ferromagnetic resonance and resistivity data show evidence for microscopic inhomogeneities, most likely antiferromagnetic LSMO, that causes FMR line broadening and a low temperature maximum in resistivity.

The research was supported by Grant No. DMR-0072144 from the National Science Foundation.

- ¹Y. Tomioka, A. Asamitsu, H. Kuwahara, Y. Moritomo, and Y. Tokura, Phys. Rev. B **53**, R1689 (1996).
- ²A. Urushibara, Y. Moritomo, T. Arima, A. Asamitsu, G. Kido, and Y. Tokura, Phys. Rev. B **51**, 14103 (1995).
- ³C. Zener, Phys. Rev. **81**, 440 (1951).
- ⁴A. P. Ramirez, J. Phys.: Condens. Matter **9**, 8171 (1997).
- ⁵M. Itoh, T. Shimura, J. Yu, T. Hayashi, and Y. Inagume, Phys. Rev. B **52**, 12522 (1995).
- ⁶G. H. Jonker, Physica (Amsterdam) **22**, 707 (1956), and references therein.
- ⁷A. K. Srivastava, C. M. Srivastava, R. Mahesh, and C. N. R. Rao, Solid State Commun. **99**, 161 (1996).
- ⁸A. H. Morrish, *The Physical Principles of Magnetism* (Wiley, New York, 1965), p. 539.
- ⁹S. E. Lofland, S. M. Bhagat, H. L. Ju, G. C. Xiong, T. Venkatesan, and R. L. Greene, Phys. Rev. B **52**, 15058 (1995).
- ¹⁰N. Zhang, W. Ding, W. Zhang, D. Xing, and Y. Du, Phys. Rev. B **56**, 8138 (1997).
- ¹¹M. Medarde, J. Mesot, P. Lcorre, S. Rosenkranz, P. Fisher, and K. Go-brecht, Phys. Rev. B **52**, 9248 (1995).
- ¹²V. Laukhin, J. Fontcuberta, J. L. Garcia-Munoz, and X. Obradors, Phys. Rev. B **56**, R10009 (1997).
- ¹³H. Y. Hwang, S.-W. Cheong, P. G. Radaelli, M. Marezio, and B. Batlogg, Phys. Rev. Lett. **75**, 914 (1995).